ADVANCED FUNCTIONAL MATERIALS

DOI: 10.1002/adfm.200500611

Multifunctional Core/Shell Nanoparticles Self-Assembled from pH-Induced Thermosensitive Polymers for Targeted Intracellular Anticancer Drug Delivery**

By *Kumaresh S. Soppimath*, *Li-Hong Liu*, *Wei Yang Seow*, *Shao-Qiong Liu*, *Ross Powell*, *Peggy Chan*, and *Yi Yan Yang**

Core/shell nanoparticles that display a pH-sensitive thermal response, self-assembled from the amphiphilic tercopolymer, poly(*N*-isopropylacrylamide-*co*-*N*,*N*-dimethylacrylamide-*co*-10-undecenoic acid) (P(NIPAAm-*co*-DMAAm-*co*-UA)), have recently been reported. In this study, folic acid is conjugated to the hydrophilic segment of the polymer through the free amine group (for targeting cancer cells that overexpress folate receptors) and cholesterol is grafted to the hydrophobic segment of the polymer. This polymer also self-assembles into core/shell nanoparticles that exhibit pH-induced temperature sensitivity, but they possess a more stable hydrophobic core than the original polymer P(NIPAAm-*co*-DMAAm-*co*-UA) and a shell containing folate molecules. An anticancer drug, doxorubicin (DOX), is encapsulated into the nanoparticles. DOX release is also pH-dependent. DOX molecules delivered by P(NIPAAm-*co*-DMAAm-*co*-UA) and folate-conjugated P(NIPAAm-*co*-DMAAm-*co*-UA)-*g*-cholesterol nanoparticles enter the nucleus more rapidly than those transported by P(NIPAAm-*co*-DMAAm)-*b*-poly(lactide-*co*-glycolide) nanoparticles, which are not pH sensitive. More importantly, these nanoparticles can recognize folate-receptor-expressing cancer cells. Compared to the nanoparticles without folate, the DOX-loaded nanoparticles with folate yield a greater cellular uptake because of the folate-receptor-mediated endocytosis process, and, thus, higher cytotoxicity results. These multifunctional polymer core/shell nanoparticles may make a promising carrier to target drugs to cancer cells and release the drug molecules to the cytoplasm inside the cells.

1. Introduction

Numerous new chemotherapeutic compounds have been developed for combating cancer. However, medical advancements have been limited because of the serious side effects caused by many of these compounds. Most anticancer drugs are taken up nonspecifically, by all types of cells. Therefore, an ideal delivery carrier for an anticancer drug should be able to transport the drug specifically to the cancer cells and release the drug molecules inside the cells, at the site where their pharmacological activity is desired. Polymeric core/shell nanoparticles have emerged recently as promising colloidal carriers for targeting poorly water-soluble and amphiphilic drugs as well as genes to tumor tissues.[1–3] Using these nanoparticles, drug targeting to solid cancers can be achieved passively by an enhanced permeability and retention effect, because of the hyperpermeable angiogenic vasculature of solid cancers.[4] Drug targeting can also be achieved by using a polymer sensitive to the surrounding temperature or pH.[5–8] Moreover, active drug targeting can be realized by attaching biological signals to the surface of nanoparticles, including antibodies, hormones, peptides, and small compounds such as folic acid that can recognize cancer cells.[9,10] Compared to antibodies, hormones, and peptides, folic acid is less expensive, more easily conjugated to the nanoparticles, and more stable during transportation, storage, and use. Unlike the other ligands listed, folate is nonimmunogenic because it is naturally found in the body.[11] More importantly, the folate receptor is frequently expressed on the surface of many human cancer cell types, and cell uptake of folate–drug conjugates or folate-conjugated nanocarriers is based on folate-receptor-mediated endocytosis. In a recent paper, we reported pH-triggered, thermally responsive core/shell nanoparticles self-assembled from the amphiphilic tercopolymer poly(*N*-isopropylacrylamide-*co*-*N*,*N*-dimethylacrylamide-*co*-10-undecenoic acid) (P(NIPAAm-*co*-DMAAm-*co*-UA)).[12] These nanoparticles exhibited a pH-dependent lower critical solution temperature (LCST). In a normal physiological environment (pH 7.4), the LCST of the nanoparticles was well

[*] Dr. Y. Y. Yang, Dr. K. S. Soppimath, L.-H. Liu, S.-Q. Liu, R. Powell, Dr. P. Chan
Institute of Bioengineering and Nanotechnology
31 Biopolis Way, The Nanos, 04-01, 138669 (Singapore)
E-mail: yyyang@ibn.a-star.edu.sg
W. Y. Seow
Department of Materials Science and Engineering
National University of Singapore
Blk EA, 07-40, 9 Engineering Drive 1, 117576 (Singapore)

[**] This work was funded by the Institute of Bioengineering and Nanotechnology, Agency for Science, Technology and Research, Singapore. We thank Prof. P. S. Low (Purdue University, USA) for valuable discussions on cancer cells that over express folate receptors. We also acknowledge the technical assistance and contribution of Chengwen Tan (Institute of Bioengineering and Nanotechnology). Supporting Information is available online from Wiley InterScience or from the author.

above normal body temperature (37 °C), and the nanoparticles were thus well dispersed. However, in an acidic environment (i.e., endosomes or lysosomes) the LCST was below 37 °C, leading to the deformation and precipitation of the core/shell nanoparticles and to the eventual release of enclosed drug molecules. In this study, cholesterol was grafted to the hydrophobic segment of P(NIPAAm-*co*-DMAAm-*co*-UA) to improve the hydrophobicity of the core of the nanoparticles so that highly hydrophobic anticancer drugs, such as paclitaxel, can be easily encapsulated. In addition, folic acid was conjugated to the free amine group of P(NIPAAm-*co*-DMAAm-*co*-UA). The resulting amphiphilic copolymer could self-assemble into core/shell nanoparticles in aqueous solution, having a shell containing folic acid molecules. These nanoparticles also exhibited a pH-dependent LCST. Doxorubicin (DOX) was used as a model anticancer drug. 4T1 mouse mammary carcinoma cells and human oral epidermal carcinoma KB cells were employed as folate-receptor-expressing cells, and A549 human lung carcinoma cells were used as folate-receptor-deficient cells. The DOX-loaded core/shell nanoparticles with folate were much more cytotoxic to 4T1 and KB cells than DOX-loaded P(NIPAAm-*co*-DMAAm-*co*-UA) nanoparticles without folate. However, the cytotoxicity of both types of nanoparticles against A549 cells was similar. Uptake of DOX-loaded nanoparticles with or without folate by folate-receptor-expressing cells was based on folate-receptor-mediated endocytosis or a nonspecific endocytosis mechanism, respectively. After endocytic uptake of nanoparticles with or without folate, DOX molecules were able to escape from the endosomes or lysosomes and enter the cell nucleus as fast as free DOX. However, more DOX molecules were taken up by the folate-receptor-expressing cells using the nanoparticles with folate. These multifunctional polymer core/shell nanoparticles may make a promising carrier for delivering anticancer drugs to cancer cells and releasing the drug molecules inside the cells to the cytosols.

2. Results and Discussion

2.1. Synthesis and Characterization of Polymers

P(NIPAAm-*co*-DMAAm-*co*-UA) polymer (feed ratio of NIPAAm/DMAAm/UA = 3.75:1.25:0.5) was first synthesized by radical copolymerization using the redox couple ammonium persulfate (APS) and 2-aminoethanethiol hydrochloride (AET·HCl).[1] Next, the carboxylic acid group of the copolymer was activated with *N*-hydroxysuccinimide (NHS), and then the activated polymer was further treated with cholesterol to yield cholesterol-grafted P(NIPAAm-*co*-DMAAm-*co*-UA). Finally, NHS-activated folic acid was coupled with the amine group of the cholesterol-grafted P(NIPAAm-*co*-DMAAm-*co*-UA) to obtain folate-conjugated P(NIPAAm-*co*-DMAAm-*co*-UA)-*g*-cholesterol (Scheme 1). The success of the copolymerization of NIPAAm, DMAAm, and 10-undecenoic acid was evidenced by the absence of vinylic proton signals at $\delta = 5.4$–6.6 ppm in the ^{1}H NMR spectrum of P(NIPAAm-*co*-DMAAm-*co*-UA). The broad peaks at $\delta = 1.5$–1.9 ppm (a + a′, Scheme 1) and at $\delta = 2.1$–2.6 ppm (b + b′, Scheme 1) were attributed to the protons of the –C*H*$_2$– and –C*H*– groups in the NIPAAm and DMAAm moieties, respectively. Other proton signals assigned to the isopropyl groups (–C*H*Me$_2$ at $\delta = 4.0$ ppm and –CH*Me*$_2$ at $\delta = 1.15$ ppm, c and d, respectively, Scheme 1) and –N*Me*$_2$ groups at $\delta = 2.9$ ppm (e, Scheme 1; Me: CH_3) were also observed, and their chemical shifts were similar to those of the monomers. From the integration ratio of signal d to signal e, the *m*/*n* ratio (unit number of NIPAAm/unit number of DMAAm) was estimated, and it was

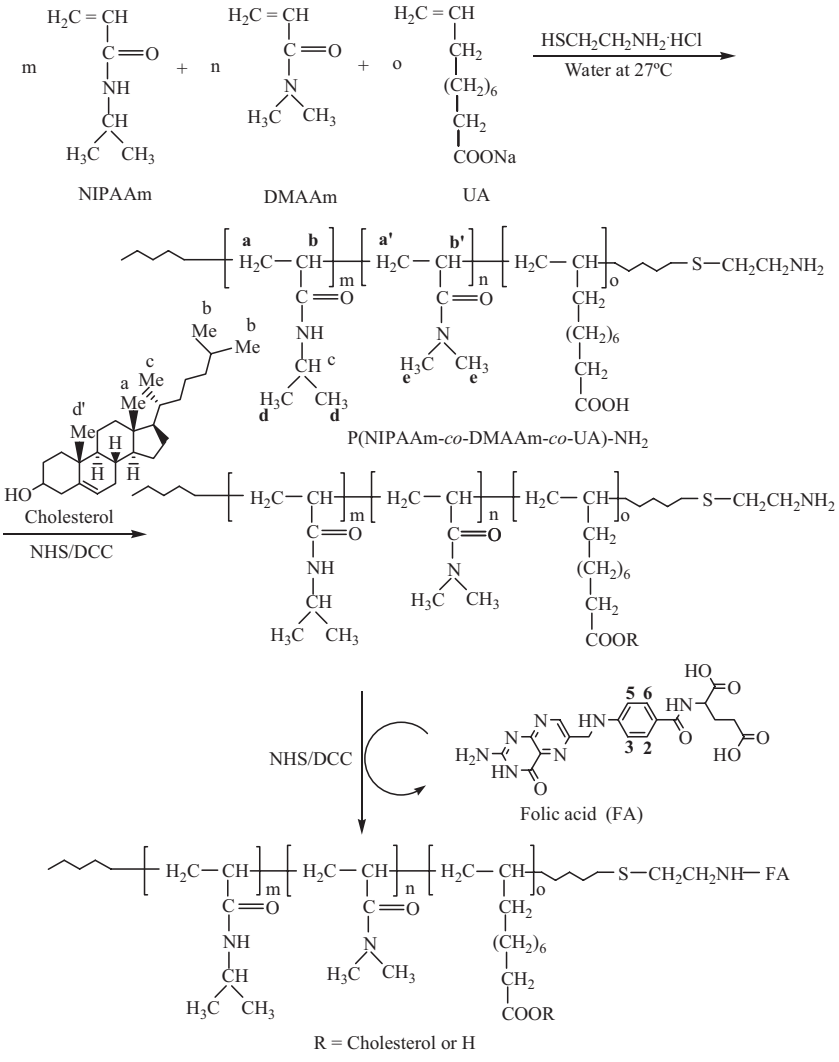

Scheme 1. Synthesis of folate-conjugated P(NIPAAm-*co*-DMAAm-*co*-UA)-*g*-cholesterol. DCC: *N*,*N*′-dicyclohexylcarbodiimide.

approximately equal to the feed ratio of the two monomers. The Fourier transform IR (FTIR) spectrum of the polymer exhibited strong absorptions at about 1645 cm^{-1} ($\nu_{C=O}$) and 1546 cm^{-1} (ν_{C-N}) from the NIPAAm and DMAAm segments. The $\nu_{C=O}$ absorption of the 10-undecenoic acid segments appeared at about 1711 cm^{-1}. The weight-average molecular weight (M_w) of P(NIPAAm-*co*-DMAAm-*co*-UA) was about 9.3 kDa. The UA content was estimated to be 44.2 mg g^{-1} of P(NIPAAm-*co*-DMAAm-*co*-UA) by acid–base titration.

Folic acid and cholesterol were successfully conjugated to P(NIPAAm-*co*-DMAAm-*co*-UA); this was confirmed by the ^1H NMR spectrum of the final polymer. The success of the conjugation of folic acid was evidenced by the presence of a broad proton signals at $\delta = 6.8–7.2$ and $\delta = 8.1–8.3$ ppm assigned to the folate aromatic protons (2,6) and (3,5) (see Scheme 1), respectively. The conjugation of the cholesterol onto the polymer was also evidenced by proton signals at $\delta = 0.66–1.2$ ppm from the five CH_3 groups in the cholesterol unit (signals a, b, c, and d′; Scheme 1). The amount of cholesterol in each polymer molecule was estimated on the basis of the integral ratio between signal d from NIPAAm and signal a from cholesterol, and the molecular weight of the polymer as well as the unit number *m* of NIPAAm, indicating that one molecule of cholesterol was attached to each polymer molecule. The average number of folate groups in each polymer molecule was estimated to be 1.2 by UV spectroscopy (UV-vis spectrometer, UV-2501PC, Shimadzu) using folic acid as the standard compound.

2.2. Critical Aggregation Concentration and LCST of Core/Shell Nanoparticles

The critical aggregation concentration (CAC) of the polymer was analyzed by fluorescence spectroscopy using pyrene as the probe. A higher peak ratio of the intensity of the third band (391 nm, I_3) to the first band (371 nm, I_1) of pyrene, I_3/I_1, obtained from the emission spectra of pyrene was observed when pyrene was located in a more hydrophobic environment.[13]

This property of pyrene can be utilized to study core/shell nanoparticle formation and deformation. The CAC of the polymer was determined to be approximately 31 mg L^{-1} in phosphate buffered saline (PBS; pH 7.4). At concentrations above the CAC, the polymer self-assembled into core/shell nanoparticles. It was noticed that the change in I_3/I_1 after the formation of folate-conjugated P(NIPAAm-*co*-DMAAm-*co*-UA)-*g*-cholesterol core/shell nanoparticles was much greater than that of P(NIPAAm-*co*-DMAAm-*co*-UA) nanoparticles (Fig. 1), suggesting the formation of a more hydrophobic core. This is attributed to the presence of the cholesterol segment of the polymer. The LCSTs of the core/shell nanoparticles in buffer solutions of different pH were determined by monitoring the change in the optical transmittance as a function of temperature. The nanoparticles were fabricated by a membrane dialysis method using dimethylacetamide (DMAc) as a solvent against buffers such as neutralized phthalate buffer (pH 5.0) and PBS (pH 6.0, 6.6, and 7.4). All the buffers were prepared with an ionic strength of 154 mM. Optical transmittance of the core/shell nanoparticles was measured at 550 nm using a UV-vis

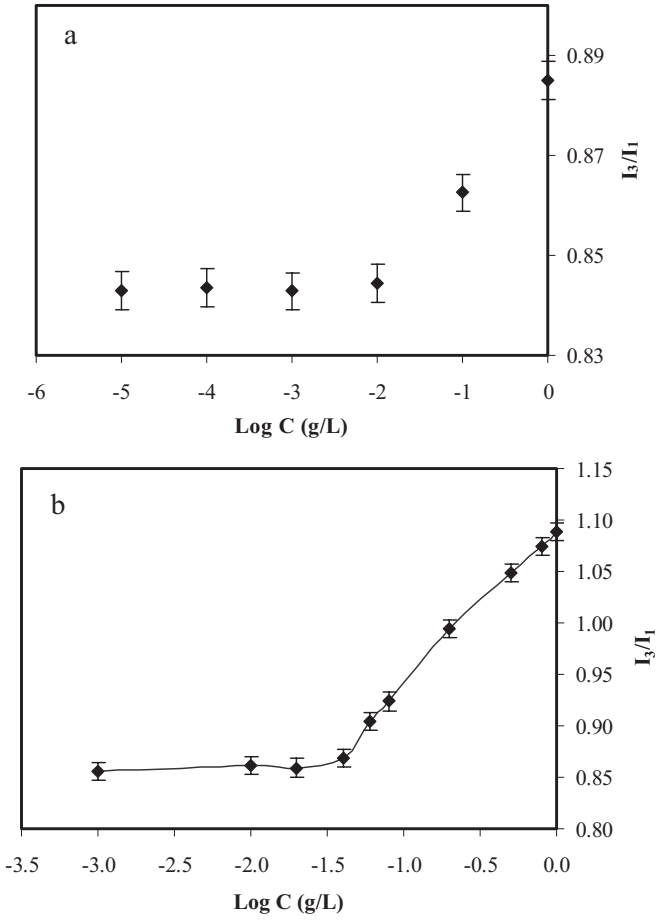

Figure 1. Plot of I_3/I_1 as a function of a) P(NIPAAm-*co*-DMAAm-*co*-UA) and b folate-conjugated P(NIPAAm-*co*-DMAAm-*co*-UA)-*g*-cholesterol concentration (*C*).

spectrometer with the sample cell thermostatted by a temperature controller (TCC-240A, Shimadzu). The heating rate was set at 0.1 °C min^{-1}. The LCST values of the core/shell nanoparticles were determined at the temperatures showing an optical transmittance of 50 % (Fig. 2). The LCST of the core/shell

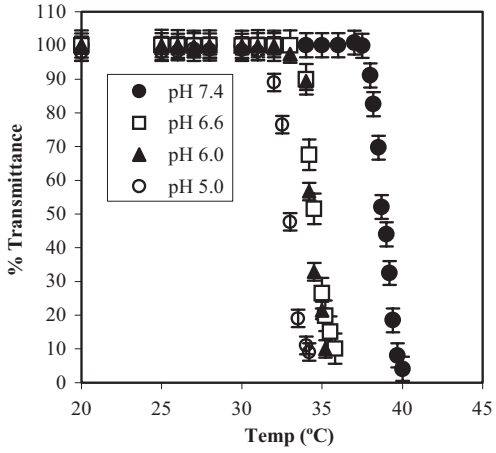

Figure 2. Plot of transmittance of core/shell nanoparticle solutions as a function of temperature, at 550 nm and various pH.

nanoparticles was pH-dependent. For instance, at pH 7.4, the LCST was 38.8 °C, well above normal body temperature (37 °C). However, at pH 6.6, 6.0, and 5.0, the LCSTs reduced to 34.5, 34.3, and 33.0 °C, respectively, much lower than 37 °C. Upon increasing the pH of the external environment, the carboxylic acid groups in the 10-undecenoic acid segment and folate were more easily deprotonated; thus, increasing the hydrophilicity of the polymer. This would lead to an increase in the LCST of the polymer, and hence that of the nanoparticles.[12]

2.3. Effect of pH on in vitro Release of DOX

Like P(NIPAAm-*co*-DMAAm-*co*-UA), folate-conjugated P(NIPAAm-*co*-DMAAm-*co*-UA)-*g*-cholesterol self-assembles into core/shell nanoparticles and also exhibits pH-dependent thermal response characteristics. We then investigated the effect of the external pH on the drug-release rate from the nanoparticles. DOX was encapsulated into the nanoparticles by membrane dialysis. Briefly, DOX (5.0 mg) was dissolved in DMAc (3 mL), and polymer (15 mg) was then added to the drug solution. The mixture was dialyzed against deionized water (500 mL) for 48 h. The DOX-loaded nanoparticles were filtered and freeze-dried. The DOX-loaded nanoparticles were smaller than 200 nm. The actual loading level of DOX in the nanoparticles was about 3.5 % by weight. In vitro drug-release studies of the nanoparticles were performed under physiological conditions (PBS, pH 7.4) and in a slightly acidic environment (pH 5.0 and 6.6) to simulate the pH of the endosomal and lysosomal microenvironments. The release profiles of DOX are shown in Figure 3. The drug release at pH 7.4 and 37 °C was considerably slow, with an initial burst of about 19 %, and only 25 % of the drug released after 48 h. In contrast, the drug release was much faster at pH 5.0 and 6.6 at 37 °C, with approximately 64 and 54 %, respectively, of the drug released within 48 h. In addition, it was observed that the drug-loaded nanoparticles were well dispersed in the buffer at pH 7.4, but aggregated and settled at the bottom of the dialysis bag at pH 5.0 and 6.6. The change in pH from 7.4 to 5.0 or 6.6 led to the deformation and precipitation of the core/shell nanoparticles, thereby causing the release of the enclosed drug. These findings are in agreement with those reported previously with P(NIPAAm-*co*-DMAAm-*co*-UA).[12]

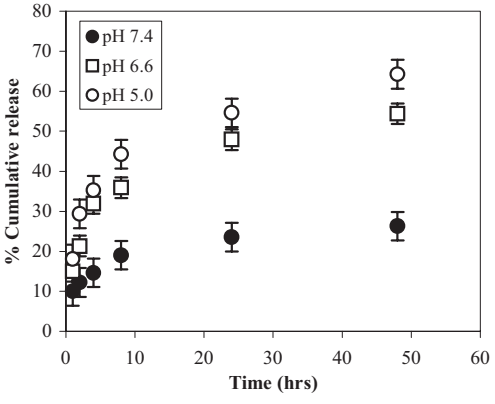

Figure 3. Release profiles of DOX from the core/shell nanoparticles at 37 °C, at varying pH.

2.4. Cellular Uptake and Cytotoxicity of DOX-Loaded Nanoparticles

The cellular uptake of DOX-loaded folate-conjugated P(NIPAAm-*co*-DMAAm-*co*-UA)-*g*-cholesterol nanoparticles by 4T1 cells (folate-receptor-expressing cells) was studied by confocal laser scanning microscopy (CLSM) and compared with free DOX, DOX-loaded P(NIPAAm-*co*-DMAAm-*co*-UA), and P(NIPAAm-*co*-DMAAm)-*b*-poly(lactide-*co*-glycolide) (P(NIPAAm-*co*-DMAAm)-*b*-PLGA)[14] nanoparticles, to understand the effects of folate and pH sensitivity. 4T1 cells were incubated with folate-free Roswell Park Memorial Institute (RPMI) 1640 medium containing free DOX (30 mg L^{-1}) or DOX-loaded nanoparticles (DOX concentration: 30 mg L^{-1}) for two hours. The samples were visualized by CLSM at an excitation wavelength of 532 nm and emission wavelength of 617 nm. All the observations were conducted under the same conditions. After two hours of incubation with free DOX, strong DOX fluorescence was observed in the cell nucleus, with no signal in the cytoplasm (Fig. 4a). For DOX-loaded P(NIPAAm-*co*-DMAAm)-*b*-PLGA nanoparticles without pH sensitivity and folate, DOX fluorescence was observed mainly in the cytoplasm instead of the nucleus (Fig. 4b). In sharp contrast, strong fluorescence was found in both the cytoplasm and the nucleus for DOX-loaded P(NIPAAm-*co*-DMAAm-*co*-UA) nanoparticles (Fig. 4c). The nanoparticles might be taken up by the cells through a nonspecific endocytosis mechanism.[15] In the endosomes and lysosomes, where the pH ranges from 4.0 to 6.5,[16] the core/shell structure of the nanoparticles might have deformed, releasing the enclosed drug molecules. On the other hand, the nanoparticles absorbs protons, and the shell of the nanoparticles becomes hydrophobic in these environments, causing an increase in endosomal/lysosomal membrane permeability and thus promoting the transportation of DOX molecules into the cytoplasm. Therefore, compared to P(NIPAAm-*co*-DMAAm)-*b*-PLGA nanoparticles, P(NIPAAm-*co*-DMAAm-*co*-UA) nanoparticles provide a better chance for DOX molecules to traffic into the nucleus. A similar phenomenon was observed for DOX-loaded folate-conjugated P(NIPAAm-*co*-DMAAm-*co*-UA)-*g*-cholesterol nanoparticles (Fig. 4d). More interestingly, the intensity of DOX fluorescence in the cells was stronger compared to the cells incubated with DOX-loaded P(NIPAAm-*co*-DMAAm-*co*-UA) nanoparticles. The cellular uptake of the nanoparticles with folate is based on a folate-receptor-mediated endocytosis mechanism[17] that might result in a greater number of nanoparticles internalized.

Cytotoxic effects of DOX, DOX-loaded P(NIPAAm-*co*-DMAAm-*co*-UA), and folate-conjugated P(NIPAAm-*co*-DMAAm-*co*-UA)-*g*-cholesterol nanoparticles were studied against 4T1, KB, and A549 cells. It should be mentioned that no obvious cytotoxicity of blank P(NIPAAm-*co*-DMAAm-*co*-UA) and folate-conjugated P(NIPAAm-*co*-DMAAm-*co*-UA)-

ADVANCED FUNCTIONAL MATERIALS

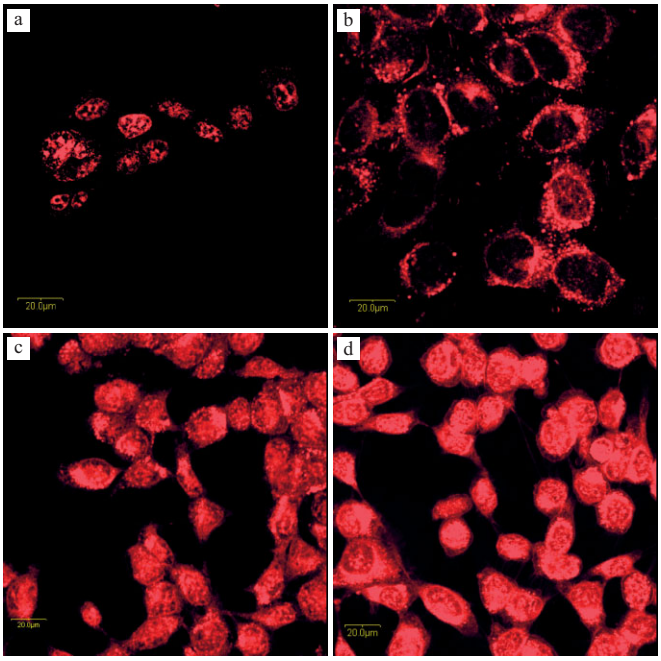

Figure 4. CLSM images of 4T1 cells incubated with a) free DOX, b) DOX-loaded P(NIPAAm-*co*-DMAAm)-*b*-PLGA nanoparticles, c) DOX-loaded P(NIPAAm-*co*-DMAAm-*co*-UA) nanoparticles, and d) DOX-loaded folate-conjugated P(NIPAAm-*co*-DMAAm-*co*-UA)-*g*-cholesterol nanoparticles at 37 °C for two hours. (DOX concentration = 30 μg mL^{-1}; all scale bars represent 20 μm.)

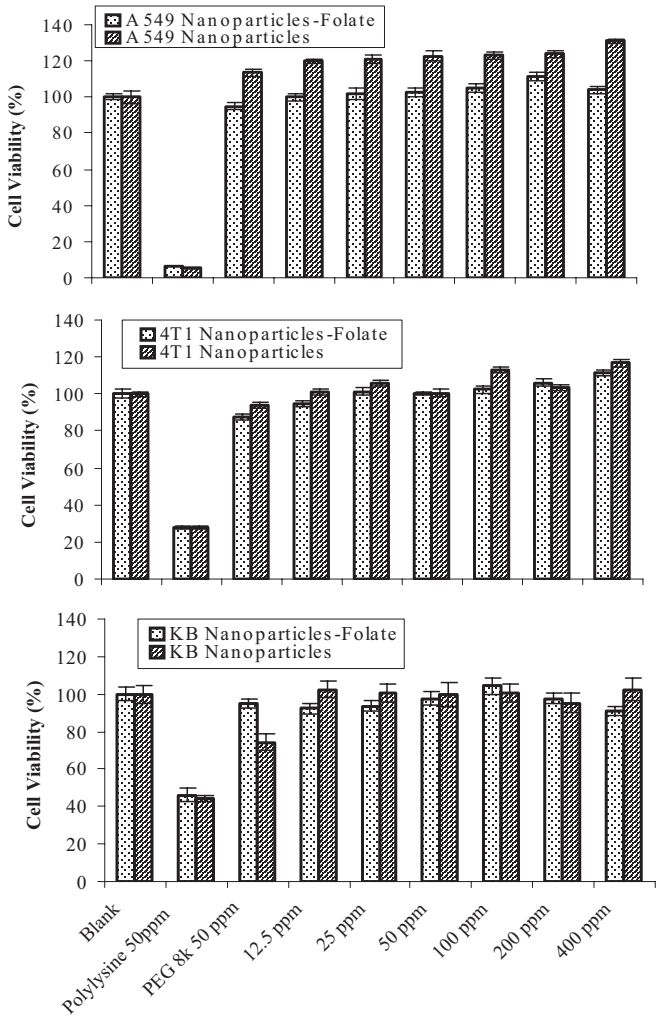

Figure 5. Cytotoxicity of P(NIPAAm-*co*-DMAAm-*co*-UA) nanoparticles (Nanoparticles) and folate-conjugated P(NIPAAm-*co*-DMAAm-*co*-UA)-*g*-cholesterol nanoparticles (Nanoparticles–Folate) against A549, 4T1, and KB cells at the concentrations specified.

g-cholesterol nanoparticles was observed in 4T1, KB, or A549 cells (Fig. 5). The cytotoxicity of DOX-loaded nanoparticles with or without folate was similar against A549 cells, lower than that of free DOX (Fig. 6a). The IC50 value of DOX, a concentration at which 50 % cells are killed, was 2.7, 3.3, and 1.4 ppm (i.e., milligrams per liter) for DOX-loaded nanoparticles with folate and without folate, and free DOX, respectively. However, the cytotoxicity of DOX-loaded nanoparticles with folate against 4T1 and KB cells was much greater than DOX-loaded nanoparticles without folate, slightly greater than free DOX (4T1 cells, IC50: 2.6, 6.9, and 2.8 ppm, respectively; KB cells, IC50: 0.48, 2.0, and 0.86 ppm, respectively) (Fig. 6b and c). This is because the folate-receptor-mediated endocytic uptake of the nanoparticles was more specific, leading to greater cellular uptake of DOX and thus killing the cells more efficiently. On the other hand, it is known that KB cells express higher levels of folate receptor than 4T1 cells. The increase in cytotoxicity against KB cells, induced by the DOX-loaded nanoparticles with folate, was much higher than that provided by the DOX-loaded nanoparticles without folate (1.6 vs. 3.2 times lower IC50).

2.5. Folate Competition

In order to further evaluate the role of folate in the cellular uptake of DOX-loaded folate-conjugated P(NIPAAm-*co*-DMAAm-*co*-UA)-*g*-cholesterol nanoparticles, the cells were incubated with the nanoparticles in RPMI 1640 medium containing increasing concentrations of free folate. The cytotoxicity of DOX-loaded nanoparticles with folate against 4T1 and KB cells was inhibited by excess free folate, and the cell viability increased with increasing folate concentration (Fig. 7). However, their cytotoxicity against A549 cells did not change as a function of folate concentration. For instance, the cell viability of DOX-loaded nanoparticles against 4T1 cells was about 63 % at DOX and free folate concentrations of 2.5 and 2.0 ppm, respectively, but it was about 100 % in the presence of 500 ppm free folate. Although there was an enhanced cell proliferation in the presence of free folate, the inhibition of cell growth significantly exceeded it (38 % inhibition versus 26 % increase at folate concentration of 500 mg L^{-1}). The cell viability of DOX-loaded nanoparticles against KB cells was approximately 20 % at a DOX concentration of 1.0 ppm, but it was about 44 % in the presence of 500 ppm free folate. These findings suggest that free folate molecules prevent the cellular uptake of the nanoparticles by competitive binding to the folate receptors on the cell surface.

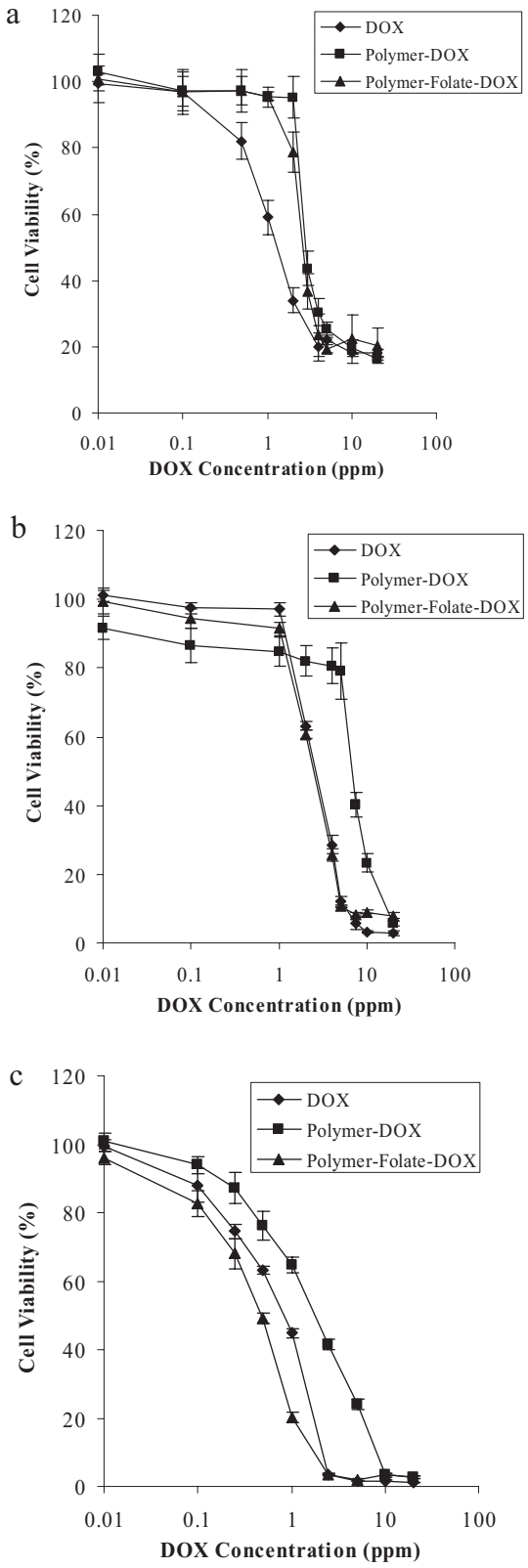

Figure 6. Viability of a) A549 cells, b) 4T1 cells, and c) KB cells after incubation with DOX, DOX-loaded P(NIPAAm-*co*-DMAAm-*co*-UA) (Polymer-DOX), and DOX-loaded folate-conjugated P(NIPAAm-*co*-DMAAm-*co*-UA)-*g*-cholesterol (Polymer-Folate-DOX) nanoparticles at 37 °C for 48 h.

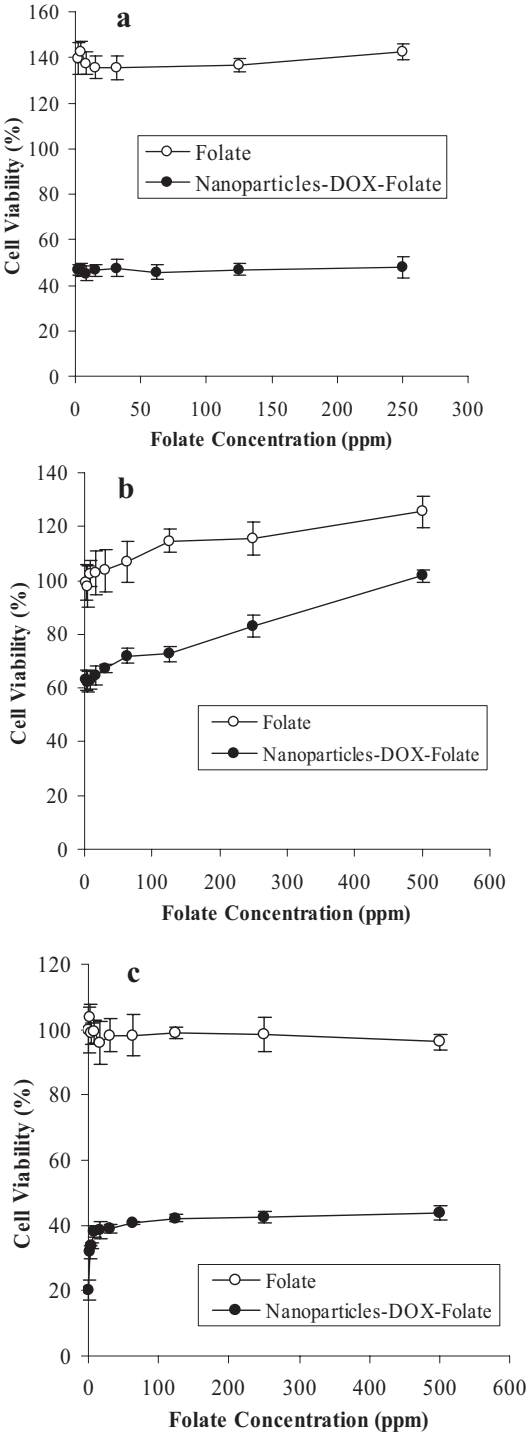

Figure 7. Effect of free folate on viability of a) A549, b) 4T1, and c) KB cells incubated with DOX-loaded nanoparticles with folate at DOX concentrations of 3.0, 2.5, and 1.0 ppm, respectively.

3. Conclusion

Novel multifunctional core/shell nanoparticles self-assembled from folate-conjugated P(NIPAAm-*co*-DMAAm-*co*-UA)-*g*-cholesterol nanoparticles have been synthesized. These

ADVANCED FUNCTIONAL MATERIALS

nanoparticles exhibited pH-triggered thermal response characteristics, are stable in PBS (pH 7.4) at 37 °C, but are deformed and precipitated in an acidic environment (e.g., endosomes and lysosomes), triggering the release of the enclosed drug molecules. Moreover, these nanoparticles could recognize folate-receptor-expressing cancer cells, demonstrating greater cellular uptake because of the folate-receptor-mediated endocytosis process and thus higher cytotoxicity. These multifunctional polymer core/shell nanoparticles may be used for cellular targeting of anticancer drugs to achieve better chemotherapy.

4. Experimental

Materials: Unless stated otherwise, all reagents and solvents were of commercial grade and were used as received. *N*-Isopropylacrylamide, *N*,*N*-dimethylacrylamide and, 10-undecenoic acid (98 %) were purchased from Aldrich and purified by crystallization (*n*-hexane) and reduced-pressure distillation. The chain transfer agent (CTA), AET·HCl, folic acid dihydrate, NHS, dicyclohexylcarbodiimide (DCC), DMAc, and dimethyl sulfoxide (DMSO) were obtained from Sigma–Aldrich. Trinitrobenzene sulfonate (TNBS; 1 M aqueous solution) was purchased from Fluka. DOX hydrochloride was kindly provided by Sun Pharmaceuticals, India. 3-(4,5-Dimethylthiazol-2-yl)-2,5-diphenyl tetrazolium bromide (MTT, Duchefa) was used in a 5 mg mL^{-1} PBS (pH 7.4) solution for cell quantification. The solution was filtered with a 0.22 μm filter to remove blue formazan crystals.

Synthesis of P(NIPAAm-co-DMAAm-co-UA): NIPAAm (8.5 g, 75 mmol) and DMAAm (2.47 g, 25 mmol) were added into ultrapure water (60 mL). UA (1.84 g, 10 mmol) was dissolved in an aqueous solution of NaOH (10 mL; 1 M). The two solutions were mixed and then neutralized with HCl solution to pH 6.6 to 6.8. The solution was purged with nitrogen gas for 15–30 min. APS (0.508 g, 2.22 mmol) dissolved in ultrapure water (5 mL) was added drop by drop, followed by slow addition of AET·HCl (0.05 g, 0.44 mmol) dissolved in ultrapure water (5 mL; about 15 to 25 s between drops). The reaction mixture needed to be cooled during the addition of AET·HCl; otherwise the precipitation of the polymer would occur because of the LCST nature of poly(-NIPAAm). After the AET was added, the reaction flask was transferred to a water bath at a temperature of 27–28 °C. The reaction was performed with stirring and under a nitrogen atmosphere for 48 h. After the completion of the reaction, the polymer was precipitated and dialyzed against water for about three days followed by ethanol for about three days to remove unreacted monomer. The final product was collected after evaporation of ethanol. The molecular weight of the polymer was determined by gel permeation chromatography (GPC, Waters, polystyrene standards), using tetrahydrofuran (THF) as the mobile phase (elution rate: 1 mL min^{-1}) at 25 °C. An acid–base titration was performed to estimate the number of carboxylic acid groups. Briefly, polymer (100 mg) was dissolved in ultrapure water (10 mL) and titrated with 0.01 N NaOH using phenolphthalein as the indicator. The number of free amine groups in the polymer was estimated spectroscopically. A known amount of polymer was dissolved in an aqueous solution of sodium hydrogen carbonate (2.0 mL; 2.0 % w/v) containing TNBS (0.01 M). The solution was kept at 40 °C for 2 h, and then cooled and diluted to a specific volume. The amount of amine functional groups derivatized with TNBS in the sample was determined using a UV-vis spectrometer at 345 nm, using alanine as the standard [18]. The experiments were performed in triplicate, and the average values are presented.

Synthesis of Folate-Conjugated P(NIPAAm-co-DMAAm-co-UA)-g-cholesterol: P(NIPAAm-*co*-DMAAm-*co*-UA) (4.15 g) was dissolved in dichloromethane (DCM; 100 mL) and then bubbled with argon for 30 min. Meanwhile, NHS (36.8 mg) and DCC (52.4 mg) were separately dissolved in DCM (7 mL). DCC was first added dropwise to the polymeric solution, followed by NHS. Activation was carried out for 24 h in an inert atmosphere with continuous stirring at room temperature (22 °C). The byproduct, dicyclohexylurea, was removed by filtration. Cholesterol (0.205 g) was then dissolved in DCM (5 mL) and added dropwise to the activated polymer solution. Conjugation was allowed to take place for 48 h in an inert atmosphere with stirring. The reaction mixture was thus dialyzed against DCM (500 mL)—using a membrane having a molecular-weight cutoff of 2000 Da (Spectra/Por 7)—for five days, to remove any unreacted cholesterol and other compounds, and then dried. Next, folate (0.75 g) was dissolved in anhydrous DMSO (15 mL) and the solution was bubbled with argon for 30 min. NHS (0.364 g) and DCC (0.388 g) were separately dissolved in DMSO (3.5 mL). To activate folate, DCC was first added dropwise to the folate solution, followed by NHS. Activation was allowed to occur for 24 h in an inert atmosphere with stirring at 22 °C. The byproduct, dicyclohexylurea, was removed by filtration. Meanwhile, cholesterol-grafted polymer (2 g) was dissolved in a mixed solvent comprising DMSO (80 mL) and THF (7 mL). The activated folate was added dropwise to the cholesterol-grafted polymer solution and conjugation was allowed to take place for 48 h in an inert atmosphere with stirring at 22 °C. The reaction mixture was thus dialyzed against DMSO (500 mL)—using a membrane with a molecular-weight cutoff of 2000 Da—for five days, to remove any unreacted compounds. The external medium was transitioned to DCM to exchange the solvent inside the bag for easy evaporation later. This was done for another three days. To harvest the final polymer, DCM was allowed to evaporate at room temperature, and the product was further dried in a vacuum oven maintained at 35 °C to remove traces of solvent. P(NIPAAm-*co*-DMAAm)-*b*-PLGA, having a weight-average molecular weight of 16.1 kDa, a polydispersity index of 1.4, a molar lactide to glycolide ratio of 85:15, and a molar PLGA-to-P(NIPAAm-*co*-DMAAm) ratio of 0.6:1, was synthesized according to the processes reported previously [14].

CAC Determination: Aliquots of pyrene solutions (1.54×10^{-5} M in acetone, 400 μL) were added to 10 mL volumetric flasks, and the acetone was allowed to evaporate. Polymer solutions at concentrations ranging from 1.0×10^{-3} to 1.0 g L^{-1} were prepared in PBS (pH 7.4). 10 mL of the aqueous polymer solutions was then added to the volumetric flasks containing the pyrene residue. All the sample solutions contained excess pyrene content at the same concentration of 6.16×10^{-7} M. The solutions were allowed to equilibrate for 24 h at room temperature. Fluorescence spectra of the polymer solutions were then recorded on a LS50B luminescence spectrometer (Perkin–Elmer, USA) at room temperature. The emission spectra were recorded from 350 to 500 nm with an excitation wavelength of 340 nm. Both excitation and emission bandwidths were set at 5 nm. From the pyrene emission spectra, the intensity (peak height) ratio (I_3/I_1) of the third band (391 nm, I_3) to the first band (371 nm, I_1) was analyzed as a function of polymer concentration. The CAC value was taken from the intersection of the tangent to the curve at the inflection with the horizontal tangent through the points at low concentrations. The experiments were conducted in triplicate, and the average values are reported. The size of the core/shell nanoparticles was analyzed using ZetaPals (Brookhaven Instruments Corporations, CA, USA) equipped with a He/Ne laser beam (670 nm). Each measurement was repeated five times, and good agreement between them was found.

In vitro Release of DOX: A certain amount of DOX-loaded freeze-dried nanoparticles was dispersed in the respective buffer solution (200 μL) and allowed to stabilize for 30 min before being placed in a dialysis membrane with a molecular-weight cutoff of 2000 Da. The dialysis bag was then immersed in neutralized phthalate buffer (25 mL; pH 5.0) or PBS (pH 6.6 or 7.4) at 37 °C. The samples were drawn at specific time intervals and the drug concentration was analyzed using UV-vis spectrophotometry at 485 nm. The drug loading was calculated based on the standard curve obtained from DOX in the buffers. The in vitro release experiments were carried out in triplicate at each pH.

Cytotoxicity Study: DOX, nanoparticle, and DOX-loaded nanoparticle solutions were prepared at stock concentrations. These solutions were diluted with growth media to give DOX and the nanoparticles at various concentrations. Poly(L-lysine) and poly(ethylene glycol) (PEG; $M_w = 8$ kDa) at a concentration of 50 ppm (mg L^{-1}) were used as the positive and negative controls, respectively. 4T1, KB, and A549 cells

(ATCC, USA) were cultured in folic acid free RPMI 1640 (Invitrogen) supplemented with 10 % fetal bovine serum and 1 % L-glutamate, and were incubated at 37 °C, 5 % CO_2. The cells were seeded into 96-well plates at 10 000 cells per well. The plates were then returned to the incubator and the cells were allowed to grow to confluence. On the morning of the initiation of the tests, the media in the wells were replaced with the pre-prepared growth medium–sample mixture (100 μL). The plates were then returned to the incubator and maintained in 5 % CO_2 at 37 °C for 48 h. Each sample was tested in eight replicates per plate. Freshly prepared growth media and aliquots of MTT solution (20 μL) were used to replace the mixture in each well after 48 h of incubation. The plates were then returned to the incubator and maintained in 5 % CO_2 at 37 °C for a further three hours. The growth medium and excess MTT in each well were then removed. DMSO (150 μL) was then added to each well to dissolve the internalized purple formazan crystals. An aliquot (100 μL) was taken from each well and transferred to a fresh 96-well plate. The plates were then assayed at 550 and 690 nm. The absorbance readings of the formazan crystals were taken to be those at 550 nm subtracted from those at 690 nm. The results were expressed as a percentage of the absorbance of the blank.

Received: September 3, 2005
Revised: March 2, 2006
Published online: January 9, 2007

[1] K. Kataoka, A. Harada, Y. Nagasaki, *Adv. Drug Delivery Rev.* **2001**, *47*, 113.
[2] V. P. Torchilin, *J. Controlled Release* **2001**, *73*, 137.
[3] F. Liu, A. Eisenberg, *J. Am. Chem. Soc.* **2003**, *125*, 15 059.
[4] Y. Matsumura, H. Maeda, *Cancer Res.* **1986**, *46*, 6387.
[5] C. S. Chaw, K. W. Chooi, X. M. Liu, C. W. Tan, L. Wang, Y. Y. Yang, *Biomaterials* **2004**, *25*, 4297.
[6] S. Q. Liu, Y. W. Tong, Y. Y. Yang, *Biomaterials* **2005**, *26*, 5064.
[7] E. S. Lee, H. J. Shin, K. Na, Y. H. Bae, *J. Controlled Release* **2003**, *90*, 363.
[8] E. S. Lee, K. Na, Y. H. Bae, *J. Controlled Release* **2003**, *91*, 103.
[9] A. N. Lukyanov, T. A. Elbayoumi, A. R. Chakilam, V. P. Torchilin, *J. Controlled Release* **2004**, *100*, 135.
[10] A. P. Janssen, R. M. Schiffelers, T. L. ten Hagen, G. A. Koning, A. J. Schraa, R. J. Kok, G. Storm, G. Molema, *Int. J. Pharm.* **2003**, *254*, 55.
[11] P. S. Low, A. C. Antony, *Adv. Drug Delivery Rev.* **2004**, *56*, 1055.
[12] K. S. Soppimath, C. W. Tan, Y. Y. Yang, *Adv. Mater.* **2005**, *17*, 318.
[13] D. C. Dong, M. A. Winnik, *Can. J. Chem.* **1984**, *62*, 2560.
[14] S. Q. Liu, Y. W. Tong, Y. Y. Yang, *Biomaterials* **2005**, *26*, 5064.
[15] R. Savic, L. Luo, A. Eisenberg, D. Maysinger, *Science* **2003**, *300*, 615.
[16] R. Duncan, *Nat. Rev. Drug Discovery* **2003**, *2*, 347.
[17] R. J. Lee, P. S. Low, *J. Biol. Chem.* **1994**, *269*, 3198.
[18] S. Syder, P. Sobocinski, *Anal. Biochem.* **1975**, *64*, 284.